

A multiphysics 3D model of tissue growth under interstitial perfusion in a tissue-engineering bioreactor

Michele M. Nava · Manuela T. Raimondi ·
Riccardo Pietrabissa

Received: 19 July 2012 / Accepted: 16 January 2013 / Published online: 31 January 2013
© Springer-Verlag Berlin Heidelberg 2013

Abstract The main challenge in engineered cartilage consists in understanding and controlling the growth process towards a functional tissue. Mathematical and computational modelling can help in the optimal design of the bioreactor configuration and in a quantitative understanding of important culture parameters. In this work, we present a multiphysics computational model for the prediction of cartilage tissue growth in an interstitial perfusion bioreactor. The model consists of two separate sub-models, one two-dimensional (2D) sub-model and one three-dimensional (3D) sub-model, which are coupled between each other. These sub-models account both for the hydrodynamic microenvironment imposed by the bioreactor, using a model based on the Navier–Stokes equation, the mass transport equation and the biomass growth. The biomass, assumed as a phase comprising cells and the synthesised extracellular matrix, has been modelled by using a moving boundary approach. In particular, the boundary at the fluid–biomass interface is moving with a velocity depending from the local oxygen concentration and viscous stress. In this work, we show that all parameters predicted, such as oxygen concentration and wall shear stress, by the 2D sub-model with respect to the ones predicted by the 3D sub-model are systematically overestimated and thus the tissue growth, which directly depends on these parameters. This implies that further predictive models for tissue growth should take into account of the three dimensionality of the problem for any scaffold microarchitecture.

Keywords Multiphysics · Simulation · Tissue engineering · Tissue growth · Bioreactor · Cartilage

M. M. Nava (✉) · M. T. Raimondi · R. Pietrabissa
LaBS, Department of Chemistry, Materials and Chemical Engineering
“Giulio Natta”, Politecnico di Milano, 32, piazza Leonardo da Vinci,
20133 Milano, Italy
e-mail: nava@stru.polimi.it

1 Introduction

The limits shown by transplantation medicine have led the medical and scientific research to undertake a new direction in reconstructive surgery based on the employment of tissues engineered *in vitro*. A basic concept in the design of dynamic culture systems for *in vitro* tissue engineering is to provide a proper biochemical and biophysical microenvironment to cells (Palsson and Bhatia 2004; Haj et al. 2005; Atala et al. 2008). In scaffold-based cartilage regeneration, imposing an interstitial flow of the culture medium is found to be particularly effective (compared both to static culture and surface perfusion) in preserving cell viability, promoting cell proliferation and up-regulating the synthesis of specific proteins, characteristic to cartilaginous tissue, such as collagen-type II and glycosaminoglycans (GAGs) (Dunkelman et al. 1995; Pazzano et al. 2000; Davisson et al. 2002; Freyria et al. 2005; Hutmacher and Singh 2008). These beneficial effects are primarily related to an improved cell oxygenation and nutrition, and an adequate removal of catabolites arising from the biosynthetic cells activity. Perfusion flow also exerts a mechanobiological effect thanks to the shear stress acting on the cell membrane (Freed and Vunjak-Novakovic 2000; Guilak et al. 2005); shear stresses, if maintained in a proper physiological range (Grodzinsky et al. 2000; Silver 2006), trigger specific signalling pathways that activate the synthesis of phenotypic markers of articular cartilage, including sulphated GAG and collagen-type II (Wendt et al. 2006).

The above considerations suggest that an efficient bioreactor should be able to guarantee a balance between mass transport and cell stimulation to enhance proliferation while maintaining cell phenotype. Most biophysical variables influencing the tissue growth process, including oxygen concentration and fluid shear stresses, are not experimentally accessible at the cell level. Computational models can be used

as valuable supports for quantitative prediction of such parameters. The problem is multiphysics, as the growth process depends on various space and time-dependent biophysical variables of the cell environment, primarily mass transport and mechanical variables, all involved in the cell biological response. Thus, an essential step towards the development of functional tissues is to precisely model both the biophysical microenvironment surrounding the growing cells and the relationship between the microenvironmental field variables and the macroscopic phenomenon of tissue growth.

The biophysical cell environment at the cell scale has already been successfully modelled by detailed pore-scale computational fluid dynamic (CFD) simulations of fluid and chemical transport in tissue-engineering scaffolds, with a simplified geometry or with more realistic architectures (reconstructed from imaging techniques), populated with few living cells (Porter et al. 2000; Singh et al. 2007; Chung et al. 2008; Cioffi et al. 2008). In these models, the volume occupied by cell growth has not been included in the modelled geometry; therefore, they basically represent initial culture conditions. These multiphysics simulations are able to capture flow, pressure and concentration fields resolved at the microscopic level. In particular, they clarify how the scaffold microarchitecture influences the hydrodynamic shear stresses imposed on cells within constructs. Calculations of nutrient flow indicate that inappropriately designed dynamic culture environments lead to regions of nutrient concentration insufficient to maintain cell viability. These studies provide a foundation for exploring the effects of dynamic flow on cell function and provide an important insight into the design and optimization of 3D scaffolds at initial culture stages.

With regard to the simulation of tissue growth, there exists a less established knowledge. An approach known as multicellular simulation has been used to model the dynamics of populations of cells that migrate, collide and divide on the basis of arbitrary laws. In these models, simple rules based on cell automata are adopted to describe cell behaviour and the emergent trend of the cell populations is observed and analysed (Cheng et al. 2006, 2009; Chung et al. 2010). Simulation results show that the speed of cell locomotion modulates the rates of tissue regeneration by controlling the effect of contact inhibition; furthermore, the magnitude of cell locomotion strongly depends on the spatial distribution of the seeded cells. In these models, cells proliferate but do not synthesize extracellular matrix, so they are valid to predict cell proliferation at early culture times. Another approach consists in homogenized models of a two-phase domain: fluid and biomass, defined as a phase comprising cells and the synthesized extracellular matrix. In (Galban and Locke 1999a,b; Chung et al. 2006), the biomass growth and nutrients diffusion are modelled within a polymer scaffold, at the macro-scale level in static culture conditions. In

a recent work, a homogenized model has been proposed to predict the local biomass growth as a function of nutrient concentration and of hydrodynamic shear stresses at specific time points in culture, in a consistently coupled logic (Sacco et al. 2011). However, this model is two dimensional (2D) and cannot realistically be applied to interpret experimental results of bioreactor tissue growth. In this work, we present a multiphysics three-dimensional (3D) model for the prediction of tissue growth in a tissue-engineering bioreactor providing interstitial perfusion to a cell-populated scaffold. The engineered tissue is considered as a single phase comprising the cells and the synthesized extracellular matrix, denoted in the following as biomass. By this assumption, the specific biological cell response, including differentiation or de-differentiation, is neglected. To model the time evolution of the biomass geometry, we use a moving boundary formulation (Galban and Locke 1997) at the biomass–fluid interface; we apply periodic remeshing to adapt the computational mesh to the large deformations of the computational domain. This model is conceived as a tool to predict physical parameters occurring in a miniaturised bioreactor that our group has recently developed (Laganà and Raimondi 2012). The mini-bioreactor has been designed to provide optical accessibility to growing three-dimensional tissue, using a standard inverted phase contrast/fluorescence microscope, during actual tissue-engineering experiments. The computational model presented here is a first step towards the integration of computational predictions with experimental findings.

2 Materials and methods

2.1 Description of the reference bioreactor set-up

The experimental set-up we modelled is described in (Laganà and Raimondi 2012) and it consists of a miniaturized optically accessible bioreactor for interstitial perfusion. As schematically shown in Fig. 1, it comprises a syringe pump (Fig. 1a) able to move the medium through a gas-permeable tube system (Fig. 1b) placed inside a small cell culture incubator (Fig. 1d). After heat (Fig. 1e) and gas exchange, the culture medium (Fig. 1c) feeds the cell-seeded scaffolds, placed inside the bioreactor. The bioreactor is mounted on an optical microscope (Fig. 1f) in a configuration that allows to acquire live images through a PC (Fig. 1g) on the cell-populated scaffolds being cultured within the bioreactor chamber, to evaluate the biomass growth during culture.

The bioreactor is designed in coordination with the specific geometry of the 3D scaffolds cultured in its chambers. To ensure a strong correlation with the computational model, rapid-prototyped polystyrene scaffolds with a plasma surface treatment, custom-made by 3D Biotek, are used in the experiments. These scaffolds are not biodegradable. The scaffold

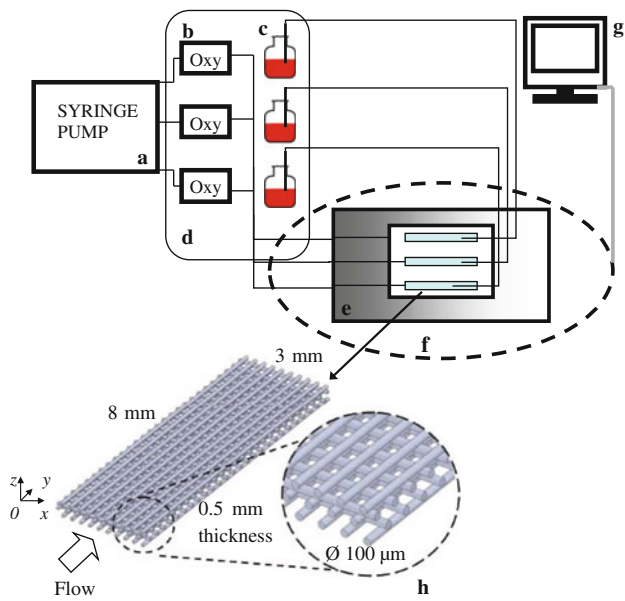


Fig. 1 Scheme of the bioreactor: **a** syringe pump, **b** oxygenator tubes, **c** culture medium reservoirs, **d** cell culture incubator, **e** heater, **f** inverted microscope and **g** monitor for the visualization of images acquired directly on the live microconstruct. **h** Microstructured scaffold designed by rapid prototyping (3DBiotek). Each cell-seeded scaffold is located in the proper canal chamber

fibres are 100 μm in diameter with a pore size of 300 μm and stacked in an offset cross-hatch geometry. The overall scaffold dimensions are 8 mm × 3 mm × 0.5 mm (Fig. 1h).

Once the bioreactor is assembled, the inlet and outlet ports are connected to the perfusion circuit and to the oxygenator tubing (DowCorning). The three independent chambers are perfused individually with complete culture medium by a syringe pump (Harvard apparatus), at a constant flow rate of 0.01 ml/min, corresponding to a mean velocity of 100 μm/s at the scaffold inlet. The resulting bioreactor is illustrated in Fig. 2a. The experimental findings relevant to the construct characterization (Fig. 2b, c) show the scaffold pores filled with the engineered tissue.

2.2 Set-up of the computational model

The computational model consists of two separate sub-models, a 2D sub-model and a 3D sub-model, which are coupled between each other. The 2D sub-model consists of a transverse section of the whole scaffold seeded with a cell monolayer and subjected to a constant interstitial (on the y-axis) flow of culture medium. The 2D sub-model, representing a slice of the full length of the scaffold, is conceived to provide realistic boundary conditions to the 3D sub-model. The geometry and the boundary conditions adopted for this 2D sub-model are shown in Fig. 3. Insulation (i.e. the normal component of the oxygen diffusive flux is null) and no-slip boundary conditions were applied to the culture chamber surfaces, under the hypothesis of impermeable and rigid

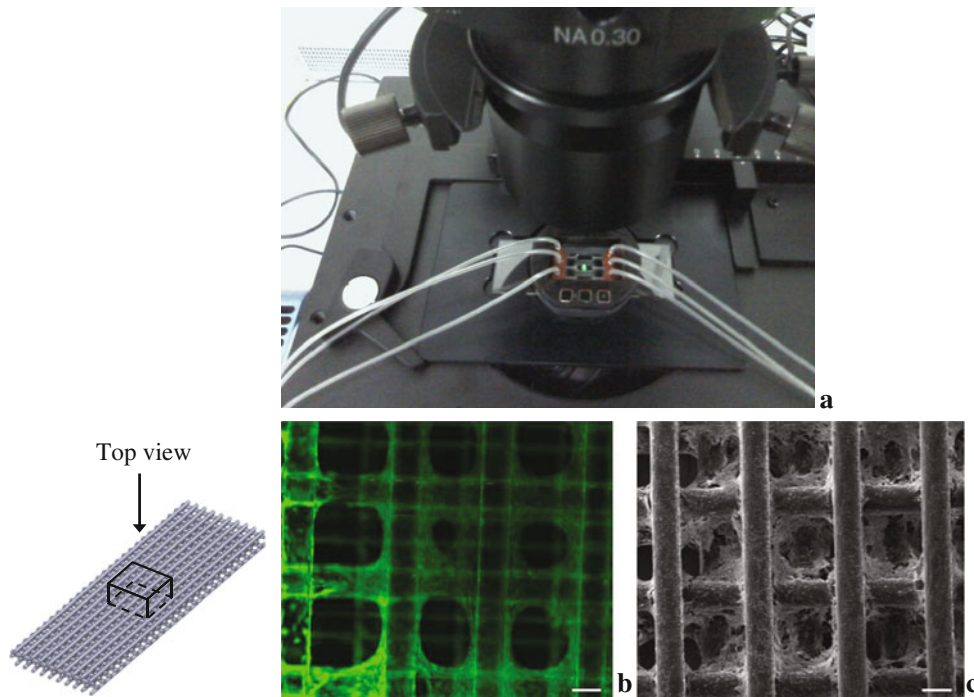


Fig. 2 **a** Bioreactor detail showing the three independent chambers connected to the perfusion chamber by oxygenator tubes; the device is placed on a standard phase contrast/fluorescence microscope. Results of the construct characterization at the end of culture. **b** Viability test, in which live cells stain green and dead cells stain red, showing the major-

ity of cells viable. **c** SEM images showing the scaffold pores filled with the engineered tissue. The scale bar is 100 μm. Reprinted and adapted from (Laganà and Raimondi 2012) with kind permission from Springer Science and Business Media

Fig. 3 2D sub-model: **a** geometry of the fibre scaffold and boundary conditions assumed for the 2D simulations; **b** detail of the mesh; the biomass is represented as a uniform and homogeneous layer of initial $4\ \mu\text{m}$ thickness. The 3D sub-model geometry is referred to the initial part of the 2D sub-model

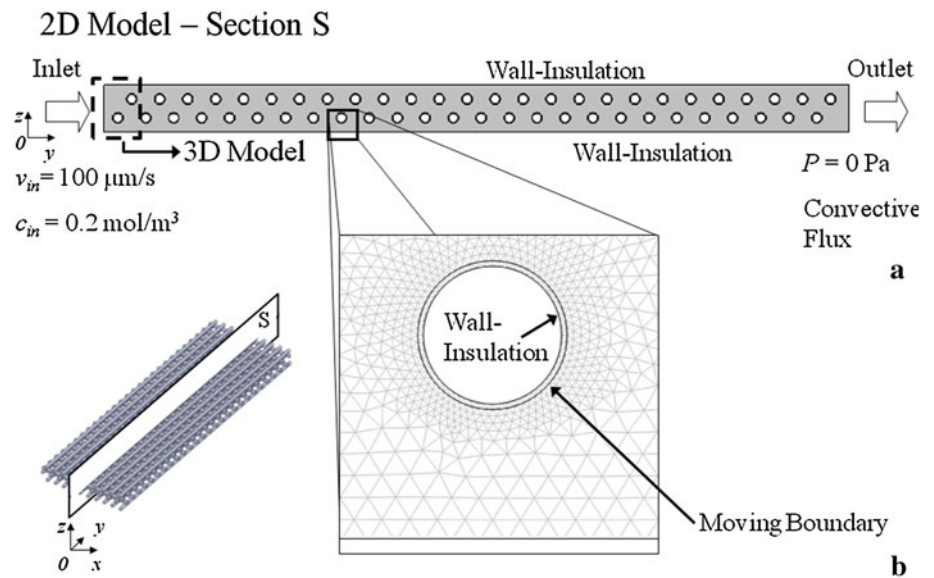
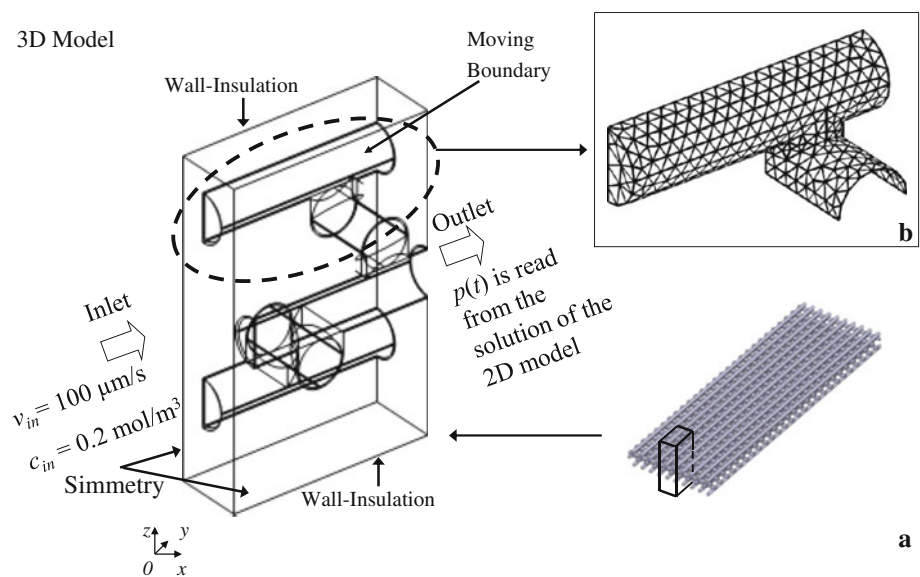


Fig. 4 3D sub-model: **a** geometry of the fibre scaffold and boundary conditions; we coupled the two sub-models: the pressures values, $p(t)$, imposed at the outlet of the 3D domain are read from the solution of the 2D sub-model at each time step; **b** detail of the mesh at the biomass sub-domain



walls. The culture medium flows in from the left of the domain and out from the right. A flat velocity profile of $100\ \mu\text{m/s}$ and an oxygen tension of $0.2\ \text{mol/m}^3$ were applied at the inlet, while a condition of null pressure and convective flux were applied at the outlet.

The 3D sub-model consists in a functional unit of the fibre scaffold (overall dimensions of $700\ \mu\text{m} \times 450\ \mu\text{m} \times 150\ \mu\text{m}$), located at the scaffold inlet. Here, a partial model of the scaffold was built by identifying the existing geometrical symmetries; the whole length of the scaffold could not be modelled due to the relevant computational cost; thus, we used the boundary conditions calculated from the 2D sub-model on our partial 3D model. The 3D sub-model geometry and boundary conditions assumed are shown in Fig. 4. Insulation (i.e. the normal component of the oxygen dif-

usive flux is null) and no-slip boundary conditions were applied to the horizontal top and the bottom domain surfaces, under the hypothesis of impermeable and rigid walls. The culture medium flows in from the left of the domain and out from the right. An oxygen tension of $0.2\ \text{mol/m}^3$ was imposed at the left of the culture chamber; a flat velocity profile of $100\ \mu\text{m/s}$ was applied at the inlet. At the outlet surface, the fluid pressure condition applied was read, at each simulation time step, from the results of the 2D sub-model, at the scaffold location corresponding to the outlet surface of the 3D sub-model. The coupling between the 2D and the 3D sub-models basically consisted in the adoption of this outlet boundary condition. A symmetry condition was assumed at the front and at the back vertical faces of the domain.

For both sub-models, the physical domains were defined as follows. The culture medium was modelled as a fluid convection-diffusion sub-domain. The fluid dynamics in the fluid domain is described by the Navier–Stokes equations (Eq. 1 and 2):

$$\nabla \cdot \mathbf{v} = 0 \tag{1}$$

$$\rho \left(\frac{\partial}{\partial t} \mathbf{v} \right) + \rho (\mathbf{v} \cdot \nabla) \mathbf{v} = \nabla \cdot (-p\mathbf{I} + \mu(\nabla \mathbf{v} + (\nabla \mathbf{v})^T)) + \mathbf{F} \tag{2}$$

where \mathbf{v} is the velocity vector, ρ is the fluid density, p is the fluid pressure, μ is the dynamic viscosity of the culture medium and \mathbf{F} is the volume forces vector. The mass transport equation in the fluid domain is the following (Eq. 3):

$$\frac{\partial c}{\partial t} - D\Delta c + \mathbf{v} \nabla \cdot c = 0 \tag{3}$$

where c is the oxygen concentration, D is the oxygen diffusion coefficient in the culture medium and \mathbf{v} is the fluid velocity predicted by Eqs. 1 and 2. The scaffold fibres are modelled as inactive domains because we assumed that the volume of the scaffold immersed in the construct is time invariant, being non-biodegradable. Thus, scaffold fibres are represented as circular/cylindrical solid domains surrounded by the biomass.

The biomass has been modelled as a solid diffusion-reaction sub-domain with oxygen volumetric consumption; we assumed that cells form a uniform and homogeneous monolayer (Freed et al. 1994), 4µm thick (Durante et al. 1993; Dorschel et al. 2002) at initial culture conditions, after the seeding procedure. The mass transport equation assumed in the biomass domain was the following (Eq. 4):

$$\frac{\partial c}{\partial t} - D\Delta c = R \tag{4}$$

where R is the biomass oxygen volumetric consumption rate, which is assumed to be a function of local oxygen concentration according to the Michaelis–Menten (M-M) kinetics (Eq. 5).

$$R = V_m \cdot \frac{c}{K_m + c} \tag{5}$$

V_m and K_m being the maximal consumption rate and the M-M constant, respectively. It has to be noted that in preliminary simulations, we had assumed the biomass as a purely elastic deformable domain. We computed fluid-induced biomass deformations which were negligible with respect to the computed biomass growth. Thus, we assumed rigid domains for the biomass in all the simulations thereon.

2.3 The biomass growth model

The interface between the biomass and the culture medium was modelled as a moving boundary (Galban and Locke

1997); this interface was assumed to be moving in time as a function of the oxygen concentration and of the fluid-induced shear stress, calculated at the surface itself. The technique used to model mesh movement was the arbitrary Lagrangian–Eulerian (ALE). The time evolution of the biomass thickness, r , was modelled by the following phenomenological law (Eq. 6)

$$\frac{\partial r}{\partial t} = f(c) \cdot g(\tau) \tag{6}$$

where τ is the fluid-induced shear stress, computed at fluid–biomass interface. Both c and τ are the function of time, t . The choice of this phenomenological law was made in order to incorporate in the model both the effects of oxygen concentration and of hydrodynamic shear on biomass growth (Fig. 5).

We assumed a modified Contois model (Contois 1959; Galban and Locke 1999a,b) for $f(c)$ (Eq. 7)

$$f(c) = K_c \cdot \frac{c}{K_d + c} \tag{7}$$

where K_c and K_d are constants. Values of these constants (Table 1) were defined by direct measurement of engineered cartilage growth on histological sections taken on a pellet model (Raimondi et al. 2011).

The function $g(\tau)$ (Eq. 8) in Eq. 6 was assumed as a modulation function, defined as:

$$g(\tau) = \begin{cases} 0.6 + 4\tau & \tau \in [0, 0.1) \text{ Pa,} \\ 1 & \tau \in [0.1, 0.6] \text{ Pa,} \\ 2.5(1 - \tau) & \tau \in (0.6, 1] \text{ Pa,} \\ 0 & \tau > 1 \text{ Pa,} \end{cases} \tag{8}$$

We assumed a beneficial effect of shear stress on tissue growth, modelled as a linear thickness increase for increasing shear stress, for values below 0.1 Pa (Raimondi et al. 2006). We assumed an harmful effect of shear stress on tissue growth at shear levels above 0.6 Pa, modelled with a linear thickness decrease for increasing shear stress, coherently with established knowledge. In the range 0.1 to 0.6 Pa, we assumed a constant value of tissue growth, since no experimental data were available for this stress range.

2.4 Computation of the solution

The commercial software Comsol Multiphysics (Comsol) was used to set-up and solve the problem and to analyse the results. The final mesh in the 2D sub-model consisted of approximately 750000 quadratic triangles, while the final mesh in the 3D sub-model consisted of 180000 linear tetrahedrons. The numerical values of the model parameters used in the simulations are referred to human chondrocytes isolated from articular cartilage and are gathered in Table 1. The simulations were run as follows. At each time point t_n , corresponding to one culture day, the solution at the previous

Fig. 5 The time evolution of the biomass thickness, r , is given by a phenomenological law (Eq. 6) consisting of the product of **a** a function of the oxygen concentration by **b** a corrective function of the wall shear stress

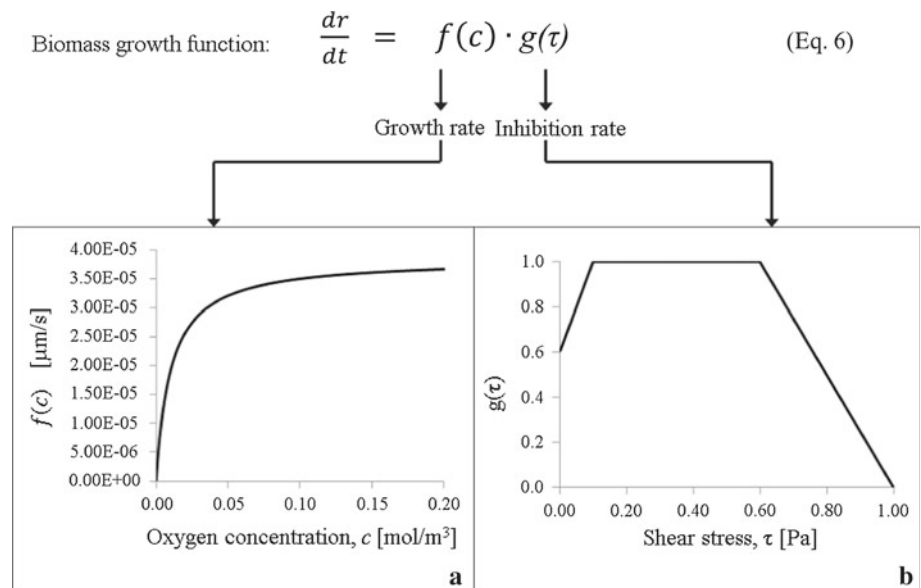


Table 1 Numerical values of the model parameters used in the simulations

Symbol	Parameters [units]	Value	Reference
μ	Fluid viscosity [Pa · s]	$8.1 \cdot 10^{-4}$	(Raimondi et al. 2002)
ρ	Fluid density at 37 °C [Kg/m ³]	1000	(Raimondi et al. 2002)
D	Oxygen diffusivity in water at 37 °C [m ² /s]	$2.1 \cdot 10^{-9}$	Palsson and Bhatia (2004)
V_m	Maximum oxygen cell consumption rate [mol/m ³ /s]	$3.84 \cdot 10^{-3}$	(Cioffi et al. 2008)
K_m	Michaelis–Menten constant [mol/m ³]	0.15	(Palsson and Bhatia 2004)
c_{in}	Oxygen concentration in the fluid at the inlet [mol/m ³]	0.2	
v_{in}	Fluid velocity at the inlet [μm/s]	100	
K_c	Maximum biomass growth velocity [m/s]	$0.385 \cdot 10^{-10}$	
K_d	Biomass growth corrective factor	0.01	

time level, t_{n-1} , was extracted from the model solution and was imposed as the initial solution to run the new simulation on the updated geometry, extracted from the deformed mesh at the previous time level, t_{n-1} , and manually re-meshed. At each time point, the following results were extracted from the simulations: the oxygen concentration field in all the active domains and the fluid velocity and shear stress fields in the fluid domain. Also, the biomass volume fraction, ε_b , was calculated at each time point, as the ratio between the biomass volume computed from the biomass thickness r and the total volume of the computational domains. The computations were run on a Windows PC with 16 Gb RAM.

3 Results

3.1 2D sub-model

The results of the 2D sub-model are shown in Fig. 6, at five simulated culture days. Oxygen concentration is progressively depleted from the medium along the flow direction (Fig. 6a), due to the consuming biomass, assumed as a solid diffusion sub-domain with oxygen volumetric consumption. The values range from a maximum saturation of 0.2 mol/m³ imposed as a boundary condition at the inlet, to the minimum value of 0.185 mol/m³ at the scaffold outlet. The shear

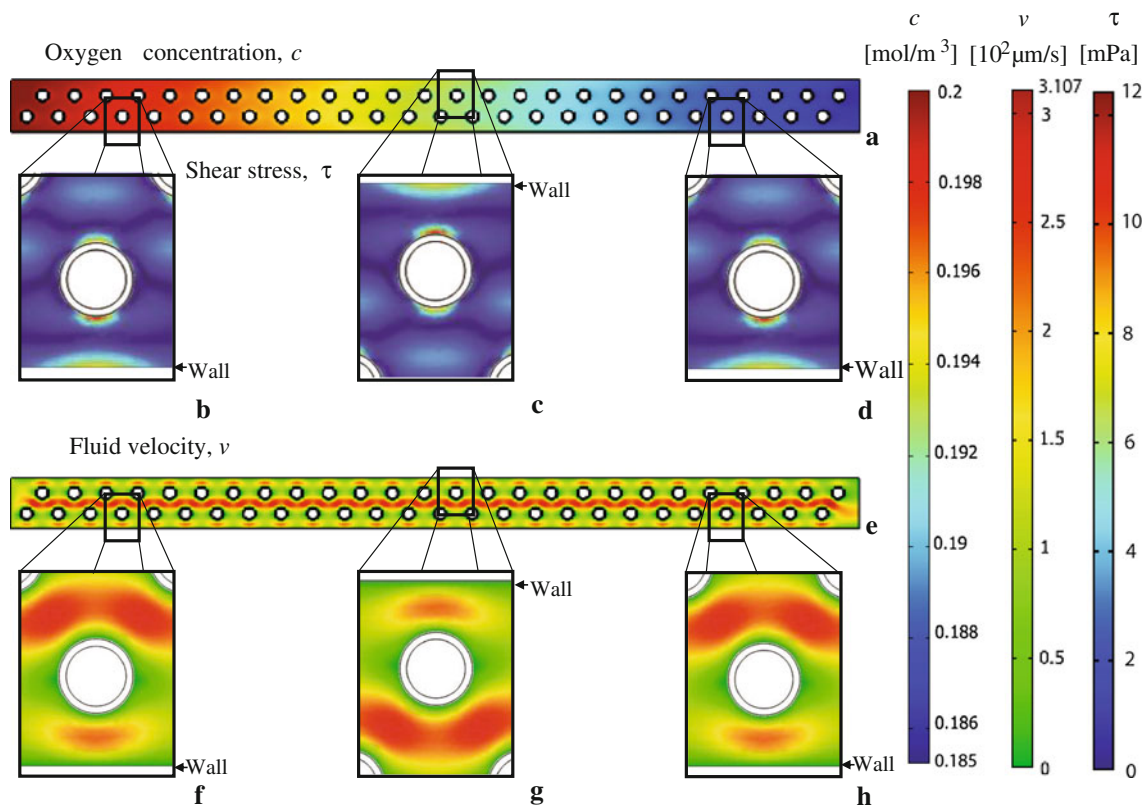


Fig. 6 Results of the 2D sub-model at five simulated culture days: **a** oxygen concentration, **b–d** fluid shear stress and **e** fluid velocity (modulus of the velocity vector) mapped on the whole scaffold and **f–h** around three representative scaffold fibres

stress in the fluid domain is mapped in the vicinity of three representative scaffold fibres (Fig. 6b–d). The stress, proportional to the velocity gradients, presents a maximum value of 12 mPa at the biomass surface. The fluid velocity field is mapped on the entire scaffold (Fig. 6e) and on three representative scaffold fibres (Fig. 6f–h). As a result of biomass growth, the velocities increase between the fibres and around those fibres located near the chamber walls. The maximum computed velocity is 311 μm/s.

3.2 3D sub-model

The results of the 3D sub-model are shown in Fig. 7, at five simulated culture days. The wall shear stress is computed at the biomass–fluid interface (Fig. 7a, b). The values increase at the superior surface of the fibres oriented perpendicularly to the flow and at the fibres intersections. The mean and maximum computed values are 4 and 14 mPa, respectively. The oxygen concentration and the fluid velocity are mapped on two sections chosen at different heights of the scaffold (Fig. 7c, d). As in 2D, oxygen concentration is progressively depleted from the culture medium along the flow direction due to biomass consumption, dropping from saturation down to a minimum value of 0.197 mol/m³ at the

domain outlet. As a result of biomass growth, the fluid velocities increase between the fibres with maximum computed values is 348 μm/s. Since the total oxygen drop within the 3D domain is only 1% and the velocity gradients are constant, the predicted biomass thickness is fairly homogeneous in this domain, in accordance with (Eq. 6).

3.3 Comparison between 2D and 3D sub-model predictions

We directly compared the mean parameter values predicted by the two sub-models, on equally dimensioned scaffold domains. The results are shown in Fig. 8 and Table 2. Oxygen tension decreases in time in both sub-models because of biomass growth (Fig. 8a). The mean oxygen concentration within the 2D sub-model is systematically higher by around 0.5% with respect to the values calculated for the microscale 3D sub-model. This is due to the fact that transverse scaffold fibres and the surrounding biomass are not considered as a computational domain in our 2D sub-model; thereby, the consumption amount related to this domain is not calculated, so the 2D sub-model simulations overestimate the mean oxygen concentration in the construct. The mean fluid velocity in both sub-models increases during culture time, as a consequence of biomass growth and of pore occlusion. Again, the

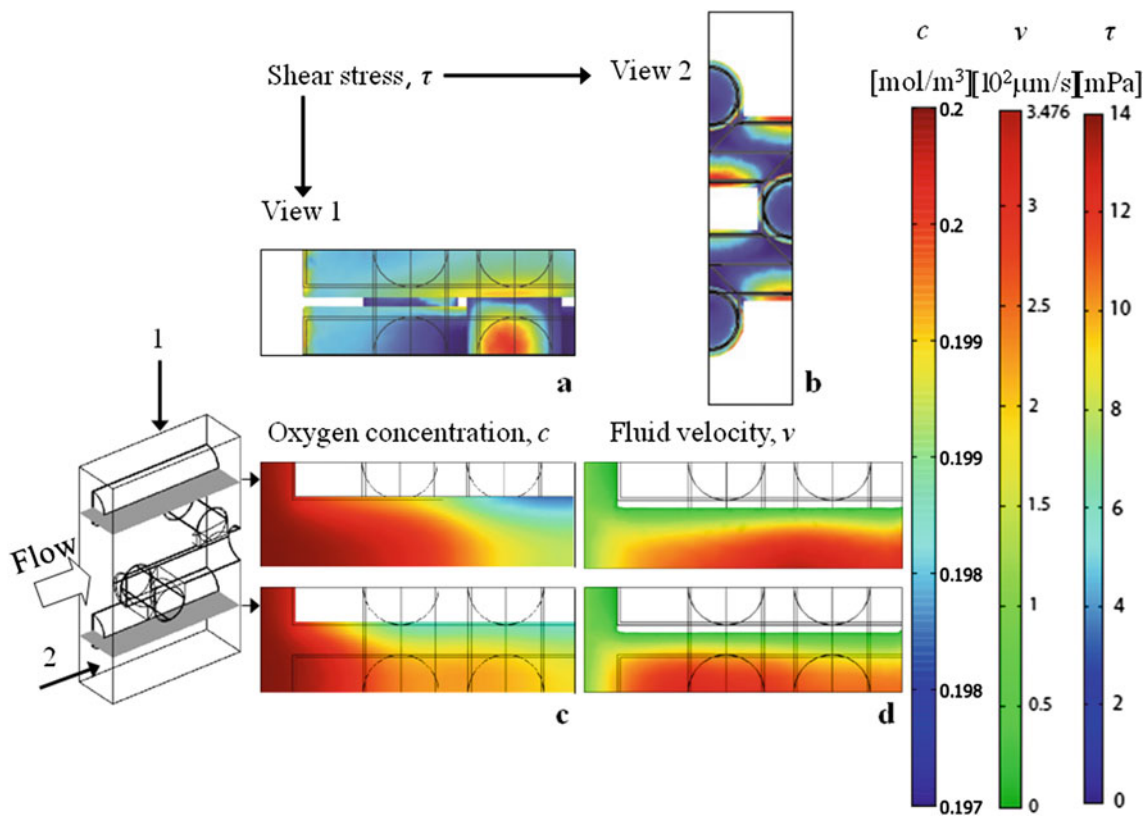
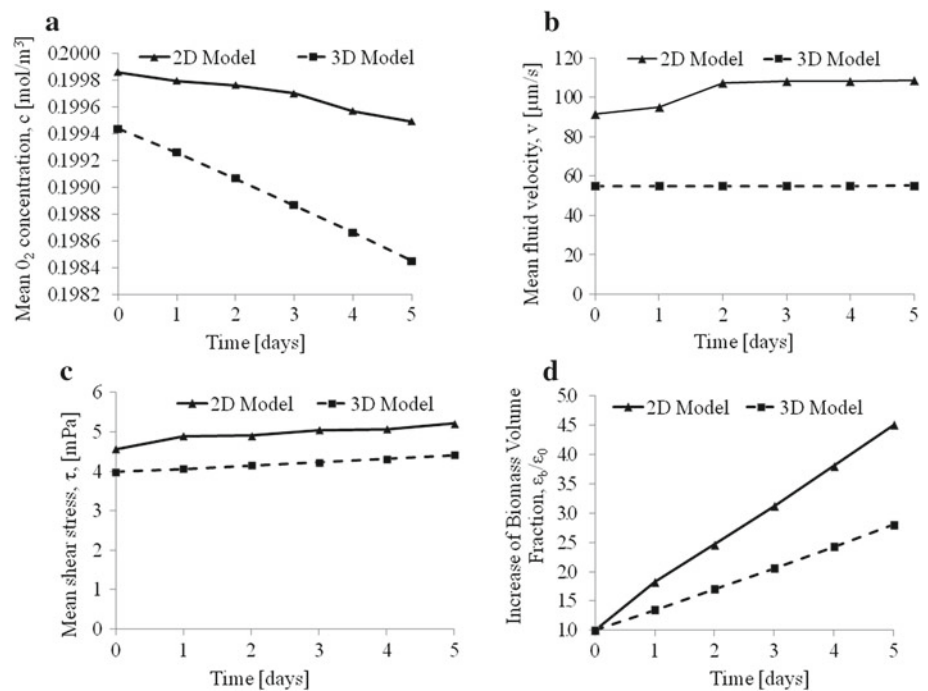


Fig. 7 Results of the 3D sub-model at five simulated culture days: **a** top view and **b** front view of the wall shear stress computed at the biomass–fluid interface; **c** oxygen concentration and **d** fluid velocity (modulus of the velocity vector) mapped on horizontal sections

Fig. 8 Comparison of results from the 2D and 3D sub-models, computed on equally dimensioned domains in the function of culture time: **a** mean oxygen concentration, **b** mean fluid velocity, **c** mean wall shear stress at the biomass surface and **d** biomass volume fraction increase with respect to the initial volume fraction, ε_0 ; $t = 0$ is equal to 1 h of simulated culture time



mean fluid velocity within the 2D sub-model is systematically higher by around 50% with respect to the values calculated for the microscale 3D sub-model, as transverse scaffold

fibres are not considered as a computational domain in 2D (Fig. 8b). The mean shear stresses at the biomass surface increase in both sub-models, consistently with the velocity

Table 2 Differences between 2D and 3D sub-model results at simulated day 5

	Difference between 2D sub-model and 3D sub-model at five simulated culture days (%)
Mean oxygen concentration, c	+0.50
Mean fluid velocity, v	+49.54
Mean shear stress, τ	+15.19
Biomass volume fraction, ε_b	+60

gradients (Fig. 8c), and the values are systematically overestimated by the 2D sub-model by around 15%. As a result of all the considerations detailed above, the biomass volume fraction is systematically overestimated by the 2D sub-model with respect to the 3D sub-model (Fig. 8d), with an overestimation error of 60% at five simulated culture days.

4 Discussion

In this work, we approached the problem of simulating tissue growth *in vitro* under interstitial perfusion by incorporating multiphysics aspects of the several interplaying processes that occur within the cell-populated construct. Three physics were considered: mass transport, fluid dynamics and biomass growth. These physics were coupled between each other in our model. Actually, at the beginning of culture, there is only a monolayer of seeded cells, which later proliferate and synthesize an extracellular matrix that changes the biomass architecture and thus the oxygen consumption. Moreover, the evolving biomass progressively restrains the flow of culture medium especially at higher biomass volume fractions. Compared to previous time-invariant pore-scale CFD simulations (Cioffi et al. 2008; Lesman et al. 2010), our model allows to take into account the space–time evolution of the engineered tissue and its surrounding microenvironment; moreover, these simulations are set-up for a well-defined scaffold architecture, but the method can be applied to any scaffold pore geometry. An important progress of our model with respect to previous ones, however, is represented by the connection between the pore-scale 3D sub-model and the 2D whole-scaffold sub-model, which allowed to define not null pressure boundary condition at the outlet for the 3D sub-model.

As for the description of the biomass growth, our approach is based on phenomenological observations: the biomass evolution in space and time is influenced primarily by two factors, oxygen concentration and fluid-induced shear stress (Schulz and Bader 2007). The influence of oxygenation on tissue growth was investigated in several numerical studies (Galban and Locke 1999a,b; Obradovic et al. 2000; Freed and Vunjak-Novakovic 2000; Cheng et al. 2006; Chung et al.

2006, 2007, 2008) but knowledge of the effect of shear stresses is still poorly understood. Our biomass growth model was based on the literature with regard to the effect of oxygen tension on tissue growth (Contois 1959; Galban and Locke 1999a,b), but we have quantified the constant parameters of the Contois model, K_m and K_d , by direct measurement of the thickening rate of cartilage pellets in bioreactor-perfused culture (Raimondi et al. 2011). This experimentally estimated growth rate was in the order of $1 \mu\text{m}/\text{day}$, that is, quite high if compared to the values adopted in previous tissue growth models (Sacco et al. 2011). As a consequence, the biomass domain changed significantly at each simulated culture time step, and we had convergence problems on the 3D sub-model solution after five simulated culture days. To model the effects of hydrodynamic stimuli on tissue growth, we introduced a phenomenological law, accounting for two phenomena: the beneficial effect of shear stress on matrix production at levels under the 10 mPa threshold (Raimondi et al. 2006) and the harmful effect at very high shear levels, which we assumed to be around 1 Pa.

It has been demonstrated that high values of hydrostatic cyclic pressure, in the order of 5–15 MPa, affect chondrocytes response by up-regulating the expression of specific cartilage marker proteins, including collagen-type II (Candiani et al. 2008). However, the level of computed static pressure exerted by the fluid flow on the growing biomass was as low as 20 Pa in our model, that is, six orders of magnitude lower than the levels able to up-regulate protein expression. Thus, the effect of static pressure induced by the fluid flow was not enough to affect biomass growth.

Our model starts with the scaffold fibres completely covered by a cell monolayer; this hypothesis is consistent with our seeding technique, consisting in a dynamic cell-seeding protocol allowing to achieve a well homogeneous cell distribution on the scaffold, before it is placed in the bioreactor for subsequent culture (Laganà and Raimondi 2012). The simulated tissue growth process within the scaffold architecture consists in the thickening of such biomass layer while invading the void space. To simulate the biomass growth, we imposed a moving boundary condition to the fluid–biomass interface (Galban and Locke 1997). The technique for mesh movement adopted is the arbitrary Lagrangian–Eulerian (ALE) method. By using this method, we could simulate the movement of the fluid–biomass interface as a function of the local oxygen concentration and of the local fluid-induced shear stress.

Our numerical predictions are in general accord with published literature with regard to the ranges of oxygen drops and shear stresses calculated at the various culture times. Also, our predicted growth rates are in general agreement with the few models published (Chung et al. 2007; Sacco et al. 2011) though only general agreement may be found in this regard, because scaffold architecture and materials, the flow rates,

cell densities and culture medium compositions differ among the various studies, and also because they are all 2D in their logic. In our work, by direct comparison of the 2D simulations with the ones from the 3D sub-model, we show that when the 3D aspects of the problem are neglected, all parameters predicted are overestimated, and therefore the tissue growth, which directly depends on these parameters through Eq. 6. This implies that the three dimensionality of the problem cannot be neglected in further tissue growth models, because, for any scaffold microgeometry, regular or irregular, any obstacle to culture medium flow perpendicular to the flow direction would be neglected in a 2D sub-model.

According to the obtained results, we can identify limitations and future developments mainly related to the 3D sub-model we proposed. Firstly, it is necessary to consider a wider 3D region in order to obtain more data on the oxygen depletion in space and time. Furthermore, the mesh deformation due to the moving fluid/biomass interface significantly influences the convergence of numerical methods used to solve the sub-models. A full-length 3D geometry and a finer mesh with quadratic elements were not possible due to the limited computing resources. Furthermore, we consider as 'biomass' a single, regular and homogeneous geometry domain but, often, during tissue-engineering experiments, the biomass does not grow homogeneously inside the scaffold architecture. The simulation of inhomogeneous seeding patterns or growth may provide useful information to guide experimentation and to interpret relevant results in these cases. As for the mass transport equations, we did not consider nutrients (e.g. glucose) and catabolites effects on biomass growth.

A further step ahead will consist in model calibration, using the bioreactor set-up modelled here.

Acknowledgments This project is funded by Politecnico di Milano, under grant 5 per Mille Junior 2009 CUPD41J10000490001 "Computational models for heterogeneous media. Application to microscale analysis of tissue-engineered constructs", by the Italian Institute of Technology (iIT-Genoa), under grant "Biosensors and Artificial Biosystems", and by the Cariplo Foundation (Milano), under grant 2010 "3D Micro structuring and Functionalisation of Polymeric Materials for Scaffolds in Regenerative Medicine".

References

- Atala A, Lanza R, Thomson J, Nerem R (2008) Principles of regenerative medicine. Academic Press, London
- Candiani G, Raimondi MT, Aurora R, Lagana' K, Dubini G (2008) Chondrocyte response to high regimens of cyclic hydrostatic pressure in 3-dimensional engineered constructs. *Int J Artif Organs* 31(6):490–499
- Cheng G, Markenscoff P, Zygorakis K (2009) A 3d hybrid model for tissue growth: the interplay between cell population and mass transport dynamics. *Biophys J* 97(2):401–14
- Cheng G, Youssef BB, Markenscoff P, Zygorakis K (2006) Cell population dynamics modulate the rates of tissue growth processes. *Biophys J* 90(3):713–724
- Chung C, Chen C, Chen C, Tseng C (2007) Enhancement of cell growth in tissue-engineering constructs under direct perfusion: modeling and simulation. *Biotechnol Bioeng* 97(6):1603–1616
- Chung CA, Chen CP, Lin TH, Tseng CS (2008) A compact computational model for cell construct development in perfusion culture. *Biotechnol Bioeng* 99(6):1535–1541
- Chung CA, Lin T-H, Chen S-D, Huang H-I (2010) Hybrid cellular automaton modeling of nutrient modulated cell growth in tissue engineering constructs. *J Theor Biol* 262(2):267–278
- Chung CA, Yang CW, Chen CW (2006) Analysis of cell growth and diffusion in a scaffold for cartilage tissue engineering. *Biotechnol Bioeng* 94(6):1138–1146
- Cioffi M, Kueffer S, Stroebel J, Dubini G, Martin I, Wendt D (2008) Computational evaluation of oxygen and shear stress distributions in 3D perfusion culture systems: macroscale and micro-structured models. *J Biomech* 41(14):2918–2925
- Contois DE (1959) Kinetics of bacterial growth: relationship between population density and specific growth rate of continuous cultures. *J Gen Microbiol* 21:40–50
- Davisson T, Sah R, Ratcliffe A (2002) Perfusion increases cell content and matrix synthesis in chondrocyte three-dimensional cultures. *Tissue Eng* 8(5):807–816
- Dorschel B, Hermsdorf D, Pieck S, Starke H, Thiele S (2002) Thickness measurements on cell monolayers using CR-39 detectors. *Nucl Instrum Methods Phys Res B*(187):525–534
- Dunkelman N, Zimmer M, Lebaron R, Pavelec R, Kwan M, Purchio A (1995) Cartilage production by rabbit articular chondrocytes on polyglycolic acid scaffolds in a closed bioreactor system. *Biotechnol Bioeng* 46(4):229–305
- Durante M, Gialanella G, Grossi GF, Pugliese M (1993) Thickness measurements on living cell monolayers by nuclear methods. *Nucl Instrum Methods Phys Res B*(73):543–549
- Freed LE, Vunjak-Novakovic G (2000) Tissue engineering bioreactors in Lanza RP, Langer R, Vacanti J. Academic Press, San Diego
- Freed LE, Vunjak-Novakovic G, Marquis J, Langer R (1994) Kinetics of chondrocyte growth in cell-polymer implants. *Biotechnol Bioeng* 43(7):597–604
- Freyria AM, Yang Y, Chajra H, Rousseau C, Ronzire MC, Herbage D, Haj AE (2005) Optimization of dynamic culture conditions: effects on biosynthetic activities of chondrocytes grown in collagen sponges. *Tissue Eng* 11(5–6):674–684
- Galban CJ, Locke BR (1997) Analysis of cell growth in a polymer scaffold using a moving boundary approach. *Biotechnol Bioeng* 56:422–432
- Galban CJ, Locke BR (1999a) Analysis of cell growth kinetics and substrate diffusion in a polymer scaffold. *Biotechnol Bioeng* 65(2):121–132
- Galban CJ, Locke BR (1999b) Effects of spatial variation of cells and nutrient and product concentrations coupled with product inhibition on cell growth in a polymer scaffold. *Biotechnol Bioeng* 64(6):633–643
- Grodzinsky A, Levenston M, Jin M, Frank E (2000) Cartilage tissue remodeling in response to mechanical forces. *Ann Rev Biomed Eng* 2(1):691–713
- Guilak F, Jones WR, Ting-Beall HP, Lee GM (2005) The deformation behavior and mechanical properties of chondrocytes in articular cartilage. *Osteoarthr Cartil* 7:59–70
- Haj AJE, Wood MA, Thomas P, Yang Y (2005) Controlling cell biomechanics in orthopaedic tissue engineering and repair. *Pathol Biol* 53(10):10
- Hutmacher DW, Singh H (2008) Computational fluid dynamics for improved bioreactor design and 3D culture. *Trends Biotechnol* 26(4):166–172
- Laganà M, Raimondi MT (2012) A miniaturized, optically accessible bioreactor for systematic 3d tissue engineering research. *Biomed Microdevices* 14(1):225–234

- Lesman A, Blinder Y, Levenberg S (2010) Modeling of flow-induced shear stress applied on 3d cellular scaffolds: implications for vascular tissue engineering. *Biotechnol Bioeng* 105(3):645–654
- Obradovic B, Meldon JH, Freed LE, Vunjak-Novakovic G (2000) Glycosaminoglycan deposition in engineered cartilage: experiments and mathematical model. *AIChE J* 46(9):1860–1871
- Palsson BO, Bhatia SN (2004) Scaling up for ex vivo cultivation. In: *Tissue engineering*. Pearson Education, London
- Pazzano D, Mercier K, Moran J, Fong S, DiBiasio D, Rulfs J, Kohles S, Bonassar L (2000) Comparison of chondrogenesis in static and perfused bioreactor culture. *Biotechnol Prog* 16(5):893–896
- Porter B, Zauel R, Stockman H, Guldberg R, Fyhrrie D (2000) 3-d computational modeling of media flow through scaffolds in a perfusion bioreactor. *J Biomech* 38(3):543–549
- Raimondi MT, Bonacina E, Candiani G, Laganà M, Rolando E, Talò G (2011) Comparative chondrogenesis of human cells in a 3Dintegrated experimental-computational mechanobiology model. *Biomech Model Mechanobiol* 10(2):259–268
- Raimondi MT, Boschetti F, Falcone L, Fiore GB, Remuzzi A, Marazzi M, Marinoni E, Pietrabissa R (2002) Mechanobiology of engineered cartilage cultured under a quantified fluid dynamic environment. *Biomech Model Mechanobiol* 1:69–82
- Raimondi MT, Moretti M, Cioffi M, Giordano C, Boschetti F, Laganà K, Pietrabissa R (2006) The effect of hydrodynamic shear on 3D engineered chondrocyte systems subject to direct perfusion. *Biorheology* 43(3–4):215–222
- Sacco R, Causin P, Zunino P, Raimondi MT (2011) A multiphysics/multiscale 2D numerical simulation of scaffold-based cartilage regeneration under interstitial perfusion in a bioreactor. *Biomech Model Mechanobiol* 10(4):577–589
- Schulz R, Bader A (2007) Cartilage tissue engineering and bioreactor systems for the cultivation and stimulation of chondrocytes. *Eur. Biophys. J.* 36:539–568
- Silver F (2006) *Mechanosensing and mechanochemical transduction in extracellular matrix*. Springer, Chap mechanochemical sensing and transduction
- Singh H, Teoh SH, Low HT, Huttmacher DW (2007) Flow modeling within a scaffold under the influence of uni-axial and bi-axial bioreactor rotation. *J Biotechnol* 119:181–196
- Wendt D, Stroebel S, Jakob M, John GT, Martin I (2006) Uniform tissues engineered by seeding and culturing cells in 3d scaffolds under perfusion at defined oxygen tensions. *Biorheology* 43(3):481–488